Embraer C-390 Millennium

Adolfo Estrada Ortiz[1]
Wentworth Institute of Technology, Boston, MA, 02115

Eduardo Meza Ubeda[2]
Wentworth Institute of Technology, Boston, MA, 02115

Britney Ruiz[3]
Wentworth Institute of Technology, Boston, MA, 02115

Figure 1: C-390 Millennium [1]

[1] Student, Mechanical Engineering, 550 Huntington Ave, Boston, MA, 02115, and University Student.

[1] Student, Mechanical Engineering, 550 Huntington Ave, Boston, MA, 02115, and University Student.

[1] Student, Mechanical Engineering, 550 Huntington Ave, Boston, MA, 02115, and University Student.

Nomenclature

A = empty weight fraction coefficient

C = empty weight fraction coefficient

E = endurance

k_{us} = sweep constant

R = range

$(L/D)_{max}$ = maximum lift-drag ratio

L/D = lift-drag ratio

v = velocity

W_o = weight of the aircraft

W_f/W_o = fuel ratio

W_{crew} = weight of crew

$W_{payload}$ = weight of payload

W_e/W_o = empty weight fraction

L_f = fuselage length

d_f = fuselage diameter

S_F = fuselage area

C_{root} = chord root length

C_{tip} = chord tip length

λ = taper ratio

$\bar{C}$ = mean aerodynamic chord

$\bar{Y}$ = location of mean aerodynamic chord

I. Introduction

The Embraer C-390 Millennium is a jet-powered military transport aircraft operated by two pilots. The first flight was done on the third of February in 2015. The manufacturer of the aircraft is Embraer Defense and Security, a Brazilian based aerospace manufacturer the makes commercial and military aircrafts. The design of the aircraft is flexible, allowing for rapid configuration changes for external and internal roles. During the first three years, the aircraft was able to accumulate 8,200 flight hours [1].

For a single aisle aircraft, there is a requirement on skin thickness necessary for an effective flight. However, the simplicity of the single aisle makes lighter metals such as aluminum a very competitive option. In recent years, composites such as carbon fiber have been used for Electromagnetic Interference Shielding. Embraer C-390 being used for military operations need the utmost reliance with their electronic equipment for things such as radar and communication systems [6]. Another reason for using carbon fiber is the advantages in its weight and cost. Unlike other industries, carbon fiber used for EMI shielding is not evaluated for its strength, just its conductivity. The Embraer C-390 non-Military applications such as humanitarian missions show the vehicles multi-purpose functionality. The aircraft is equipped with a Continuous Computed Drop Point (CCDP) algorithm that calculates the best drop point for supply deployments. Without the EMI shielding by carbon fiber, potential interference while using the CCDP would negatively impact efficiency and accuracy while trying to provide relief aid. [2]. C-390 is made of mostly carbon fiber and aluminum. Structural parts of the plane are manufactured by FAdeA in Argentina. Parts of the wings and side doors are manufactured by AERO Vodochody in Czech Republic. The Brazilian team manufacturing this plane has customers all around the world and have even discussed installing a production line of these planes in India in order to benefit both countries [3].

The total height of the aircraft is 11.84 meters, the total wingspan is 35.05 meters, and the total length is 35.2 meters. The maximum takeoff weight is 86,999kg and the fuel capacity is 23,000kg. The use of twin IAE V2500-E5 jet engines allow a cruising speed of 0.8 Mach (about 988km/hr). The aircraft's cruising speed is 870km/hr, and stall speed is 193km/hr. It also has a flight time of 7,500 hours and a travel distance of 3,000 miles. Due to the speed and the total travel time and distance, the aircraft has been allowed to travel anywhere in the world in a much faster way. The maximum payload is 26 metric tons, which provides several uses including "humanitarian support, medical evacuation (MEDEVAC), search and rescue, and aerial refueling. … deployed to transport and launch cargo and troops and perform paratroopers' operations" [4]. During the COVID pandemic, the Brazilian Air Forces used the C-390 to deliver medical supplies to remote places in the Amazon. Other countries that use this aircraft are Hungary, Netherlands, and Portugal [5].

II. Weight Calculation

To determine the weight of the Embraer C-390 Millennium an iterative calculations method was used. When looking for the lift drag ratio (L/D_{MAX}) of the Embraer C-390 aircraft, we utilized the calculated wetted aspect ratio of 4.4. This calculated value allowed us to estimate an L/D ratio of 20 for our military aircraft using Graph 1. With the L/D ratio, the weight of the fuel ratio between each stage of takeoff and landing was then determined by using Equations 1-3. The values for each of the ratios are listed in Table 1.

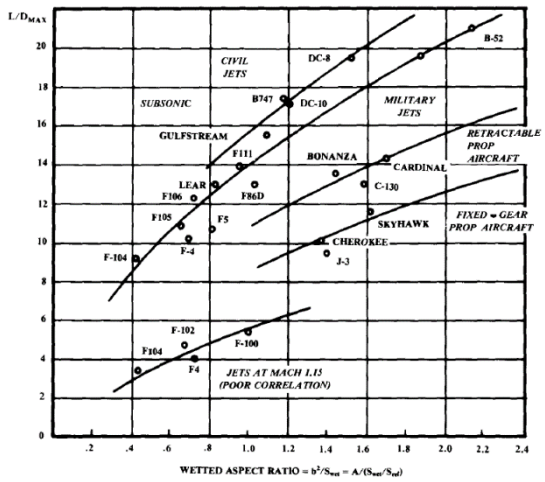

Fig. 3.6 Maximum lift to drag ratio trends.

Chart 1: L/D_{max} vs. Wetted Aspect Ratio

$$\frac{W_x}{W_o} = \frac{W_1}{W_o} * \frac{W_2}{W_1} * \frac{W_3}{W_2} * \frac{W_4}{W_3} * \frac{W_5}{W_4} \tag{1}$$

$$\frac{W_3}{W_2} = \exp\left(-\frac{RC}{V\left(L/D\right)}\right) \tag{2}$$

$$\frac{W_4}{W_3} = \exp\left(-\frac{EC}{L/D}\right) \tag{3}$$

Table 1: Fuel Weight Ratio

$\frac{W_1}{W_o}$(warmup)	$\frac{W_2}{W_1}$(climb)	$\frac{W_3}{W_2}$(cruise)	$\frac{W_4}{W_3}$(loiter)	$\frac{W_5}{W_4}$(landing)	$\frac{W_x}{W_o}$
0.97	0.987	0.8461	0.846	0.995	0.68053

$$\frac{W_f}{W_o} = 1.06 * \left(1 - \frac{W_x}{W_o}\right) = 0.3386 \tag{4}$$

Table 3.1 Empty weight fraction vs W_0

$W_e/W_0 = A W_0^C K_{vs}$	A	C
Sailplane—unpowered	0.86	−0.05
Sailplane—powered	0.91	−0.05
Homebuilt—metal/wood	1.19	−0.09
Homebuilt—composite	0.99	−0.09
General aviation—single engine	2.36	−0.18
General aviation—twin engine	1.51	−0.10
Agricultural aircraft	0.74	−0.03
Twin turboprop	0.96	−0.05
Flying boat	1.09	−0.05
Jet trainer	1.59	−0.10
Jet fighter	2.34	−0.13
Military cargo/bomber	0.93	−0.07
Jet transport	1.02	−0.06

K_{vs} = variable sweep constant = 1.04 if variable sweep
= 1.00 if fixed sweep

Using the values from the table above, we are able to determine values for A and C to use for Equation 5. The W_o from Equation 5 will be constantly changing in the iterative method in order to determine the weight of the aircraft.

$$\frac{W_e}{W_o} = A * W_o^c * k_{us} \tag{5}$$

$$W_o = \frac{W_{crew}+W_{payload}}{1-\left(W_f/W_o\right)-\left(W_e/W_o\right)} \tag{6}$$

The following shows the python code that was used to calculate the weight. It shows the while loop for the iterative calculation and the conditions that needed to be reached in order for the loop to stop and produce the final results. From research, the initial weight guess of 163,140lb was used for the iterative process. The resulting calculated weight of 193,944.163lbs was done with an error of 0.5%. This margin of error resulted in a weight difference of 30K pounds. This is similar to the weight necessary to fill the oil tank of an Embraer C-390. This makes sense since the iterative process shows the decline in aircraft weight as it takes off and uses its fuel for its flight path. The empty weight ratio (W_e/W_0), of a real Embraer C-390 would have a difference of weight of about 30K pounds when including things like the weight of the crew and/or any other equipment meant for military or civilian aid. There are variations of the Embraer C-390 that would carry more weight in fuel, however for the base multipurpose version of the plane, we can expect its weight change to behave similarly to the values found in the iterative process.

```python
#=====CONSTANTS=====#
R =  1.9061*(10**7) #(ft)
C1 = 0.0001389 #(1/sec)
V = 792 #(ft/s) crusing
E = R/V#24080.4 #2.7*(10**7) #(s)

W_crew = 640 #(lb)
#W_1 = 163140#57320.2 #(lb) payload + aircraft
We = 100000#70000#52030 #(lb)
W_pay = 50700#30865#57320.2#W_1 - We
A = 0.93
C2 = -0.07

#===DRAG LIFT RATIO===#
wing_span = 115 #(ft)
Swet = 624.17*4 +700 #(ft^2)
aspect_ratio = ( wing_span**2 )/Swet
#print(aspect_ratio)
ld_ratio_max = 13
ld_ratio = 20

W1_o = 0.97
W2_1 = 0.985
W3_2 = np.exp((-R*C1)/(V*ld_ratio))
W4_3 = np.exp(-(E*C1)/(ld_ratio))
W5_4 = 0.995
```

```python
Wx_o = W1_o * W2_1 * W3_2 * W4_3 * W5_4
Wf_o = 1.06 * (1-Wx_o)

Wo_guess = 163140#50000 #inital guess
e = 0.5
i = 1
condition = True
while condition:
    print(i)
    We_o = A*((Wo_guess)**C2)
    print('We_o is:',We_o)

    Wo = (W_crew+W_pay)/( 1 - Wf_o - We_o)


    bla = abs(Wo - Wo_guess) / Wo_guess *100
    if bla <=  e:
        condition = False
        print('Wo is:',Wo)
        print('percent error is:',bla)
    else:
        Wo_guess = Wo
        i =+ 1  # i = i + 1

```

III. Fuselage and Wing Dimensions

To calculate the fuselage dimension, the length of it needs to be calculated first by using Equation 1. Based on Table 6.3, the coefficients that were used is a=0.23 and C=0.50. Using the weight calculated previously (193,944.163lb), the length of the fuselage was determined to be 101.289ft. By rearranging Equation 8, the diameter of the fuselage was found, and Equation 9 gives the fuselage area. All the measurements for the fuselage can be found in Table 2.

Table 6.3 Fuselage length vs W_0

Length = aW_0^C	a	C
Sailplane—unpowered	0.86	0.48
Sailplane—powered	0.71	0.48
Homebuilt—metal/wood	3.68	0.23
Homebuilt—composite	3.50	0.23
General aviation—single engine	4.37	0.23
General aviation—twin engine	0.86	0.42
Agricultural aircraft	4.04	0.23
Twin turboprop	0.37	0.51
Flying boat	1.05	0.40
Jet trainer	0.79	0.41
Jet fighter	0.93	0.39
Military cargo/bomber	0.23	0.50
Jet transport	0.67	0.43

$$L_f = aW_o^C \tag{7}$$

$$\frac{L_f}{d_f} = 6 \tag{8}$$

$$S_f = \frac{\pi d_f^2}{4} \tag{9}$$

Table 2: Fuselage Dimensions

Fuselage Length (L_f)	Fuselage Diameter (d_f)	Fuselage Area (S_f)
101.289 ft	16.88165 ft	223.83075 ft

The chord root and the chord tip lengths for the wings are 21.38ft and 5.68ft, respectively. Using this and Equation 10, the taper ratio was calculated.

$$C_{tip} = \lambda C_{root} \tag{10}$$

Table 3: Wing Dimensions

Chord Root	Chord Tip	Aspect Ratio	Wingspan (b)	Taper Ratio (λ)
21.38 ft	5.676 ft	4.137	115 ft	0.26548

The means aerodynamic cord is the average chord length for a tapered swept wing and is calculated using Equation 11. The location of the mean aerodynamic chord is found using Equation 12. The angle between the leading edge and vertical line and the angle between the quarter chord line and vertical line is found using Equation 13 and Equation14 respectively.

$$\bar{C} = \frac{2}{3} C_{root} \frac{1+\lambda+\lambda^2}{1+\lambda} \tag{11}$$

$$\bar{Y} = \frac{b}{6} \frac{1+2\lambda}{1+\lambda} \tag{12}$$

$$\tan \Lambda_{LE} = \frac{C_{root}}{b/2} \tag{13}$$

$$\tan \Lambda_{0.25\bar{C}} = \frac{0.25\bar{C}}{\bar{Y}} \tag{14}$$

Table 4: Wing Dimensions Cont.

Mean Aerodynamic Cord ($\bar{C}$)	Location of Mean Aerodynamic Cord ($\bar{Y}$)	$\tan \Lambda_{LE}$	$\tan\Lambda_{0.25\bar{C}}$
71.7262	31.2528	0.27587	0.57375

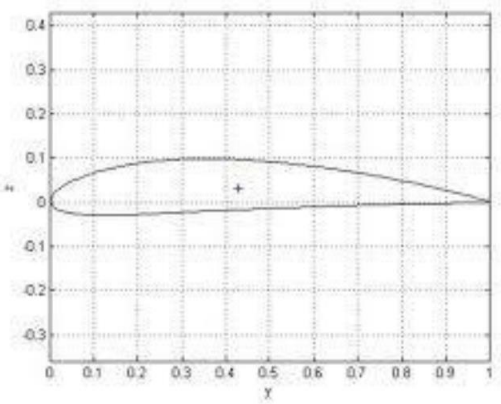

Figure 1: NACA 4412 Diagram

The airfoil for the C-390 Embraer Millennium is the NACA 4412. By using Chart 2 lift and drag coefficients for the airfoil were determined at five different angles of attack. Using Chart 3 the moment of coefficient was also determined. All these values are listed in Table 5.

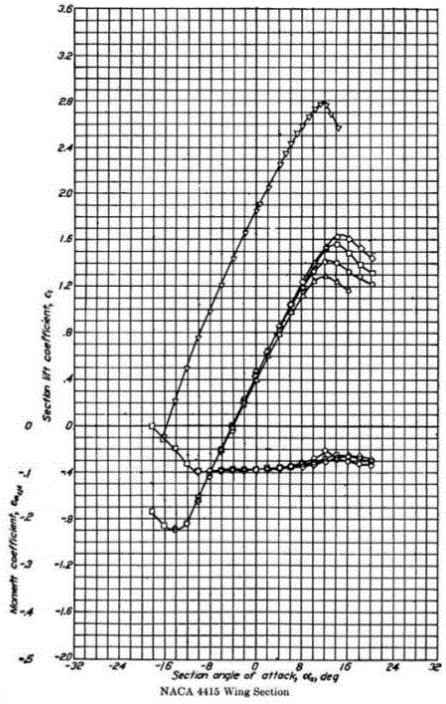

Chart 2: Angle of Attack Vs. Lift coefficient

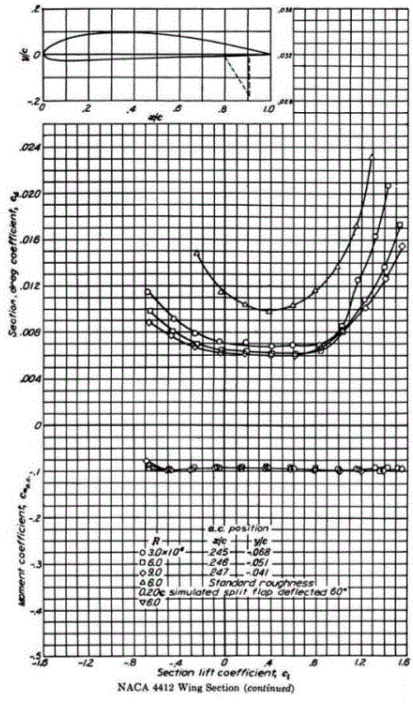

Chart 3: Lift Coefficient Vs. Drag Coefficient

Table 5: Angle of Attack Lift and Drag

Angle of attack	Lift Coefficient	Drag Coefficient	Moment of coefficient at the aerodynamic center
0	0.4	0.0069	-0.099
8	1.2	0.013	-0.099
15	1.4	0.019	-0.099
18	1.3	0.0155	-0.099
24	1.0	0.0079	-0.099

Flaps are an important part of the wing and aircraft. These devices help reduce the climb rate and decrease the stall speed during landing. The chord length and span for the flaps are found using Equations 15 and 16. The flaps generate additional lift which can be calculated by using the stall speed and take off speed (Equations 17 and 18), as seen in Equation 19.

$$C_f = 0.36 * C = 7.69ft \tag{15}$$

$$b_f = 0.67 * b = 77.05ft \tag{16}$$

$$V_s = \sqrt{\frac{2(W/S)_{wing}}{\rho C_{LMAX}}} = 27.726 ft/s \quad (17)$$

$$V_{To} = 1.2 * V_s = 33.27 ft/s \quad (18)$$

$$C_{lTO} = \frac{2*W_{TO}}{\rho * V_{TO}^2 * S} = 1.4 \quad (19)$$

Table 6: Flaps Dimensions

Flap Chord (C_f)	Flap Span (b_f)	Stall Velocity (V_s)	Take off Velocity (V_{To})	Lift Coefficient (C_{lTO})
7.69ft	77.05ft	27.726ft/s	33.27ft/s	1.4

IV. Critical Mach Number

The critical Mach number is a significant value because it is the lowest Mach number at which the airflow reaches the speed of sound. To estimate the critical Mach number for the NACA 4412 two approaches were used and compared, a graphical solution and an analytical solution.

a. Graphical Solution

Assumed for low speed, essentially incompressible flow so the pressure coefficients experience Mach numbers within a small range of anything below sonic (Ma = 1). Equation 20 is the first used to find a graphical solution for critical Mach number. The Mach numbers ranged from 0.1 < Ma < 0.99 with a constant k = 1.4. In equation 21, $c_{p,o}$ was a given value that very helpful in graphing the second airfoil Mach number equation. The range of Mach numbers are the same used to graph equation 20.

$$C_{p,cr} = \frac{2}{kMa_\infty^2}\left[\left[\frac{2+(k-1)Ma_\infty^2}{k+1}\right]^{k/(k-1)} - 1\right] \quad (20)$$

$$C_p = \frac{C_{p,o}}{\sqrt{1-Ma_\infty^2}} \quad (21)$$

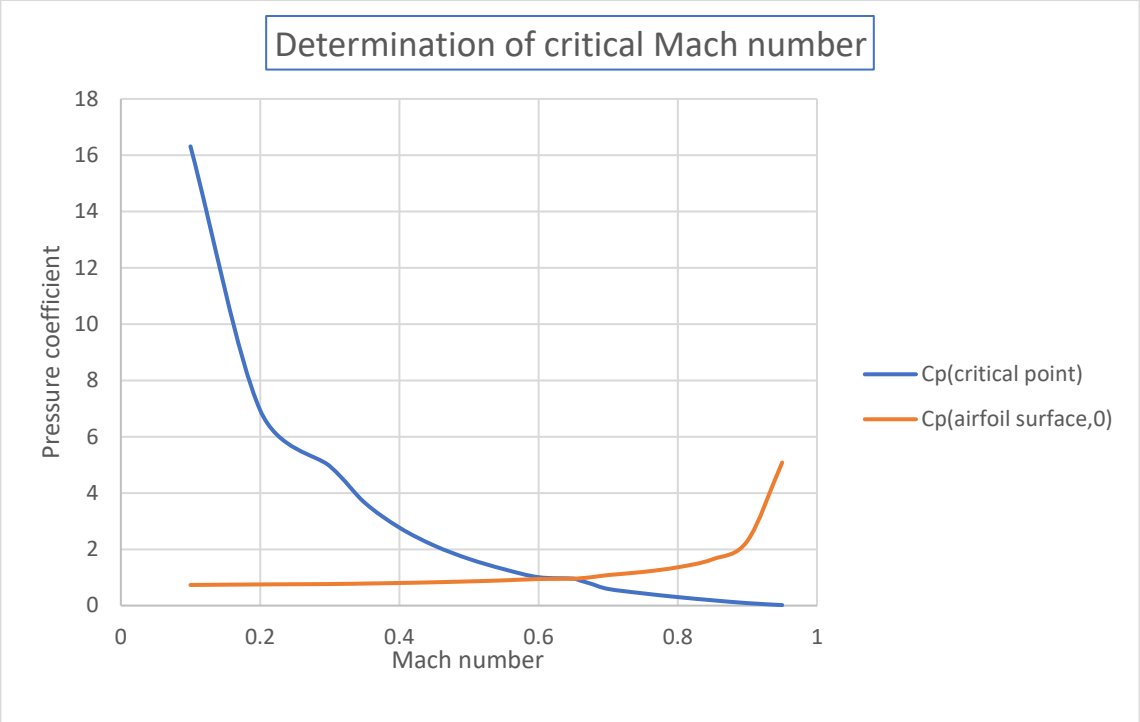

A graph of $C_{p,cr}$ vs. Mach number was plotted using equation 20 and 21, resulting in a critical Mach number of 0.65. This value is very close to the number found through the analytical solution, which assures that its representative of our aircrafts airfoil.

b. Analytical Solution

The following equation was used for the analytical approach. Different Mach numbers were used until both sides were equal. Table 7 shows the multiple Mach numbers used. From this method, we got a Critical Mach Number of 0.66 which is very similar to the Mach number obtained through the graphical approach of 0.65. The analytical solution was more accurate because of the large sample size used. The graphical solution was lacking.

$$\frac{C_{p,o}}{\sqrt{1-Ma_\infty^2}} = \frac{2}{kMa_\infty^2}\left[\left[\frac{2+(k-1)Ma_\infty^2}{k+1}\right]^{k/(k-1)} - 1\right] \tag{22}$$

Table 7: Trial and Error of Mach Number

Ma_{cr}	Left Side	Right Side
0.05	-0.717	-269.024
0.15	-0.725	-29.419
0.25	-0.7405	-10.2455
0.35	-0.765	-4.956
0.45	-0.8028	-2.772

0.55	-0.858	-1.658
0.65	-0.9435	-1.00
0.75	-1.08	-0.592
0.66	-0.954	-0.958

V. Horizontal and Vertical Stabilizer

The stabilizer plays a significant role in keeping the plane from swinging from side-to-side and up-and-down. Due to this, it is necessary to determine the dimensions for both vertical and horizontal tails. Equations 23 through 26 provides the formulas used to determine area, span and root for the vertical stabilizer. Table 8 lists all these variables.

Chart 4: Vertical Stabilizer Characteristics

No	Aircraft	Type	m_{TO} (kg)	Airfoil	$(t/C)_{max}$ (%)	$\overline{V}_V$	S_V/S	AR_V	Λ_V (deg)
1	Wright Flyer	First aircraft in history	420	Flat plate	low	0.013	0.045	6.3	0
2	Cessna 177	GA single prop engine	1,100	NACA 0009/0006	7.5	0.14	0.107	1.41	35
3	C-130 Hercules	Large turboprop cargo	70,305	NACA 64A-015	15	0.06	0.18	1.84	18.8
4	DC-9/10	Large jet transport	41,100	DSMA	11	0.08	0.19	0.95	43.5
5	Cessna Citation I	Business jet	5,375	NACA 0012/0008	10	0.0806	0.191	1.58	33
6	Fokker F-27	Turboprop transport	19,773	modified NACA	15	0.07	0.203	1.55	33
7	Boeing 737-100	Large jet transport	50,300	-	12	0.11	0.27	1.88	35
8	Beechjet 400A	Business jet transport	7,303	-	12	0.123	0.263	1	55
9	DC-8-10	Large jet transport	141,000	DSMA-111/-112	9.85	0.05	0.122	1.91	35
10	Airbus 300B	Large jet transport	165,000	-	12.5	0.102	0.204	1.623	40
11	C-17A	Heavy jet cargo	265,352	-	9	0.08	0.195	1.36	36
12	Eurofighter 2000	Fighter	21,000	-	7	0.035	0.096	1.3	45
13	F-15 Eagle	Fighter	36,741	-	7	0.06	0.346^{δ}	1.3	35

Vertical tail characteristics for several aircraft

$$S_v = (sv/s) * S \tag{23}$$

$$b_v = \sqrt{AR_v * S_v} \tag{24}$$

$$C_{rv} = 2 * \frac{S_v}{b_v(1+taper\ ratio)} \tag{25}$$

$$C_{tv} = C_{rv} * taper\ ratio \tag{26}$$

Table 8: Vertical Stabilizer Dimensions

Mean Aerodynamic Chord	Span (b_v)	Area (S_v)	Root Chord Length (C_{rv})	Tip Chord Length (C_{tv})
225.6651	29.1163	623.3525	29.5297	13.2883

The following five equations were used to determine the dimensions of the horizontal stabilizer. Table 9 lists all the variables.

Chart 5 A and B: Coefficients Used For Horizontal Stabilizer Calculations

No	Aircraft	Type	Overall length (m)	$\overline{V}_H$
1	Cessna 172	Light GA (Piston)	7.9	0.76
2	Piper PA-46-350P	Light transport (Piston)	8.72	0.66
3	Alenia G222	Turboprop transport	22.7	0.85
4	Fokker 100	Jet transport	35.5	1.07
5	Lake LA-250	Amphibian	9.04	0.8
6	Boeing 747-400	Jet transport	73.6	0.81
7	Airbus 340-200	Jet transport	59.39	1.11
8	Pilatus PC-12	Turboprop transport	14.4	1.08
9	Eurofighter 2000	Fighter	15.96	0.063
10	F/A-18	Fighter	18.31	0.49

Tail volume coefficients of several aircraft

No	Aircraft configuration/ type	*l*/L
1	An aircraft whose engine is installed at the nose and has an aft tail	0.6
2	An aircraft whose engine(s) installed above the wing and has an aft tail	0.55
3	An aircraft whose engine installed at the aft fuselage and has an aft tail	0.45
4	An aircraft whose engine installed under the wing and has an aft tail	0.5
5	Glider (with an aft tail)	0.65
6	Canard aircraft	0.4
7	An aircraft whose engine is inside the fuselage (e.g. fighter) and has an aft tail	0.3

Typical values for the l/L for various aircraft configurations

$$I = (I/L) * L \tag{27}$$

$$S_h = (V_h * C * S)/I \tag{28}$$

$$b_h = \sqrt{AR_h * S_h} \tag{29}$$

$$C_{rh} = \frac{2*S_h}{b_h*(1+taper\ ratio)} \tag{30}$$

$$C_{th} = C_{rh} * taper\ ratio \tag{31}$$

Table 9: Horizontal Stabilizer Dimensions

Aerodynamic Center (I)	Span (b_h)	Area (S_h)	Root Chord Length (C_{rh})	Tip Chord Length (C_{th})
50.643	68.5796	1147.1134	55.7557	22.3023

VI. SOLIDWORKS model

The Embraer-C390 is an oddly shaped cargo transportation with swept wings, T-Tail empennage, and a wide body that concaves horizontally. For the solid works model the aircraft was split into 4 different components. The fuselage, wings, horizontal and vertical stabilizers

were all modeled separately based off the dimensions calculated in Part III for the fuselage and wings and in Part V for the horizontal and vertical stabilizers. The plane was originally modeled in a 1:1 ratio to the real Embraer and scaled down to fit the inlet of the wind tunnel. The real wingspan is 115 feet and 5 inches (115’ 5”) which was shrunk down to a 4.14-inch wingspan.

Figure 2: Solidworks Model of C-390 Based on Calculated Values

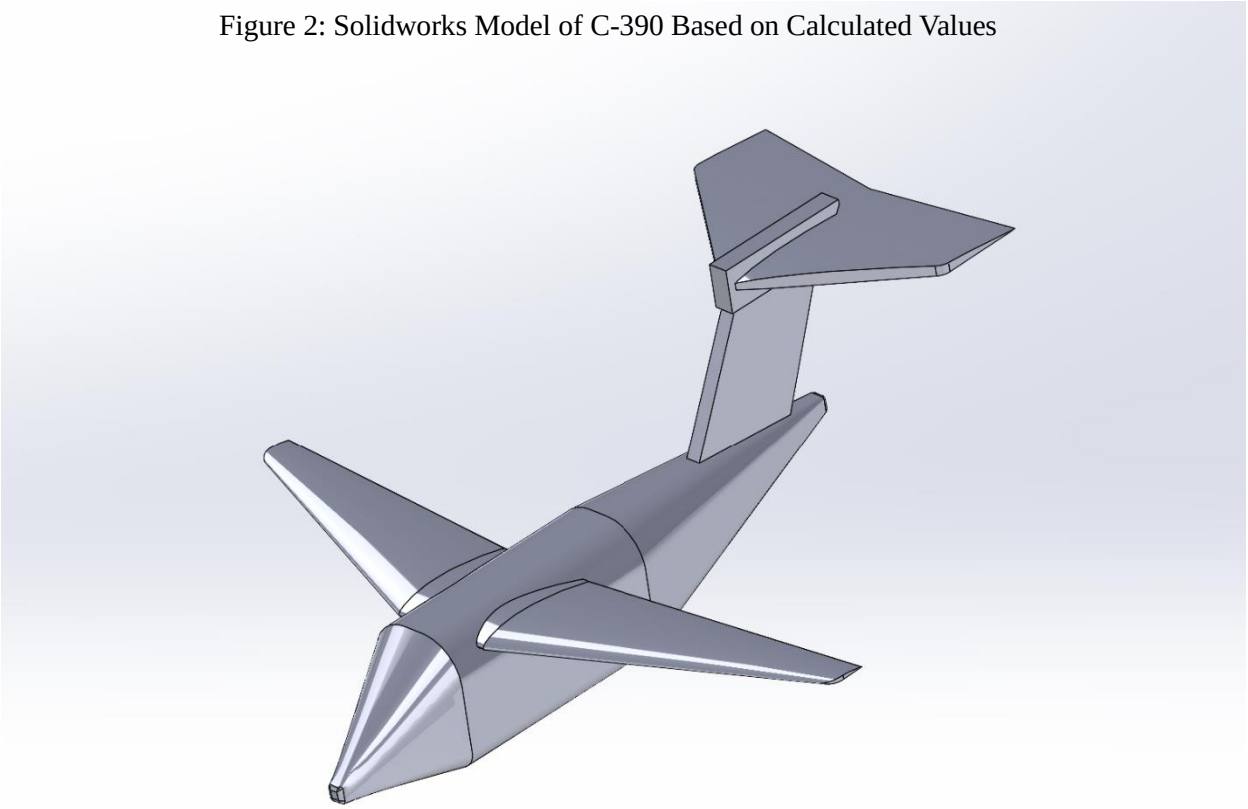

VII. Computational Fluid Dynamics Simulation Analysis

Solidworks Flow Simulation was used to perform varies CFD analysis of the aircraft at different angles of attack and speeds. The parameter (temperature, pressure, density) for each simulation was based on the conditions of the fluid lab since the data collected through the CFD will be compared to the results gathered through the wing tunnel. The temperature and pressure used were 70°F and 14.78lb_f/in^2, respectively. Three different velocities were used, 30%, 60% and 100% of the max velocity of the wind tunnel. Through the CFD analysis, the drag and lift force for each angle of attack was obtained through post-processing. The level of the initial mesh was set to 3 and offset distance for the equidistance refinement local mesh was set to 0.01ft around the plane. Figure 3 shows the convergence of the global goals (drag and lift force). After about 100 iterations, the values for the lift and drag started to converge to their respective force in pound-force.

Figure 3: Convergence Chart of Global Goals at 8° attack angle

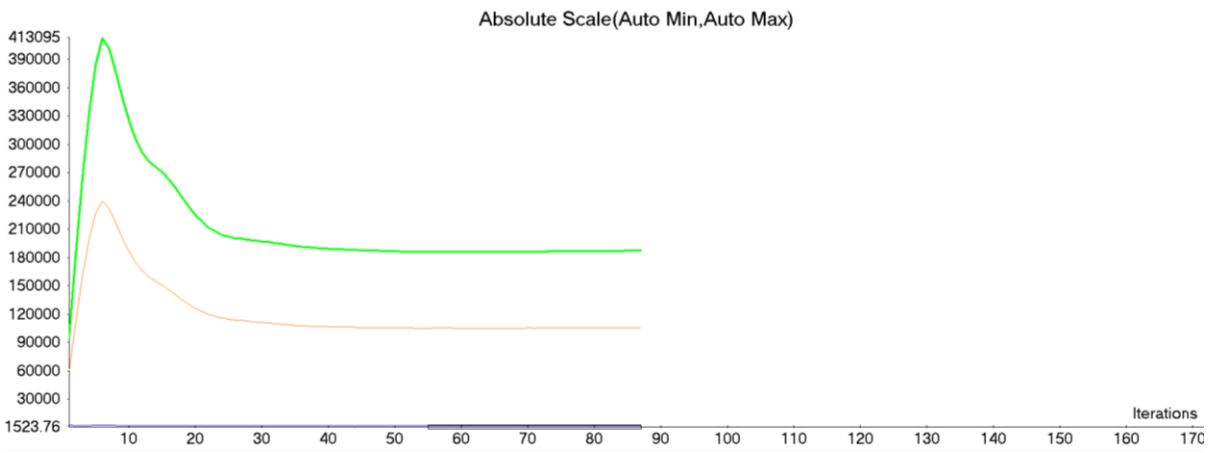

Figure 4: Mesh Cut Plot at 24°

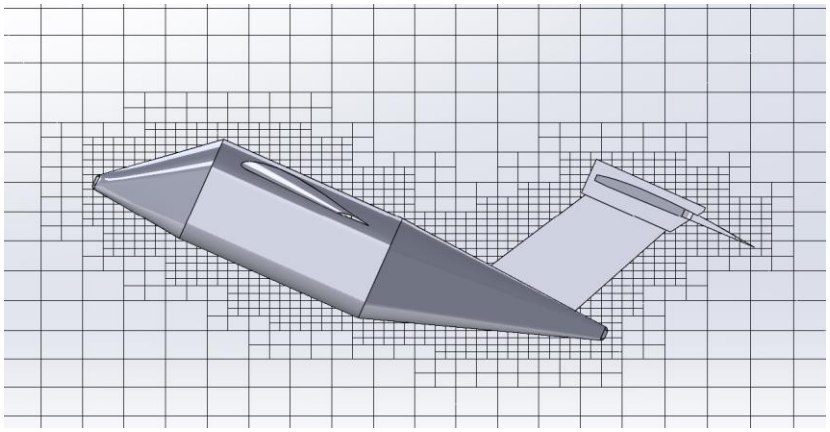

The following Mesh cut gives a spatial representation of the nodes and cells created to show the following flow simulation as well as velocity and pressure plots. The Embraer C-390 has a high hanging T-tail for its horizontal stabilizer which creates interesting fluid dynamics. The other angle of attacks would show close to same mesh cut as Figure 4, but just oriented at different pitches.

Figure 5: Flow simulation for Angle of attack of 24◦ at 60% airspeed (62.2 ft/s)

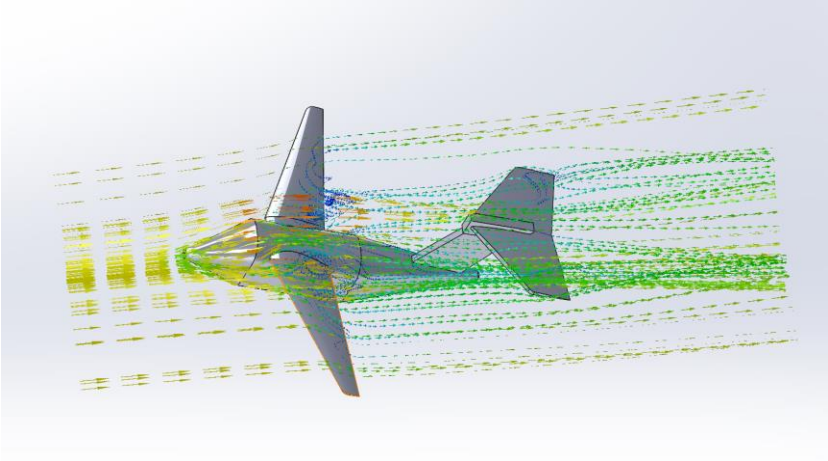

The following CFD flow is the middle speed used for simulation calculations. The 60% speed shown reveals the pressure difference needed to create a decent amount of lift, but the two different low-pressure pockets of air having different values create a little more unwanted drag for the aircraft. For 100% speed the low pressure is more equally distributed on the wings rather than the mid body. This is better because it creates a more controlled lift than drag compared to lower speeds. For the 30% airspeed there is not enough pressure difference which is why the (L/D) ratio is smaller at lower speeds.

Figure 6A and 6B: Pressure and Velocity plots for 30% airspeed (30.54 ft/s) [no attack]

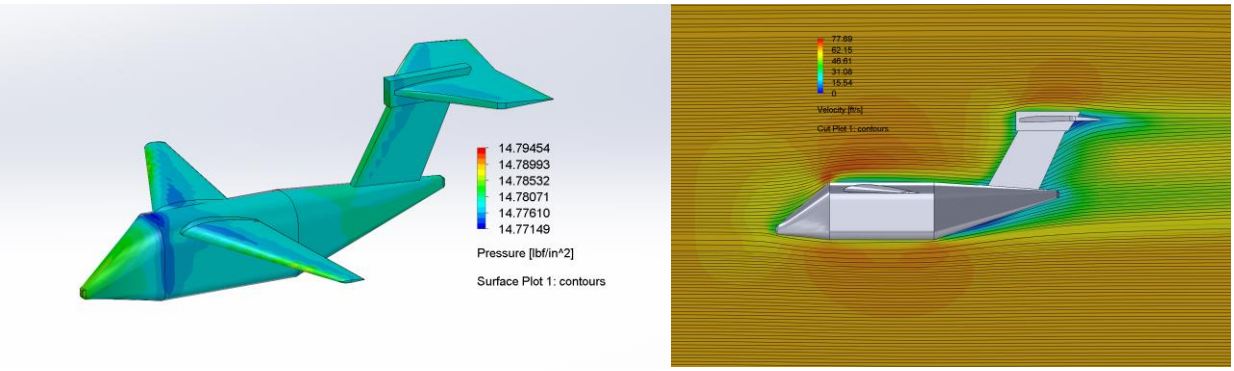

Figure 7A and 7B: Pressure and Velocity plots for 100% airspeed (30.54 ft/s) [angle of attack 24°]

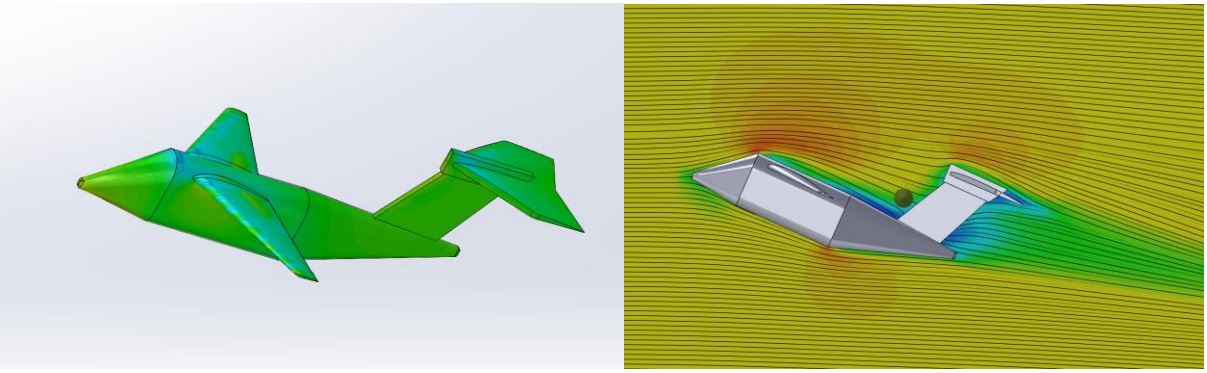

Figures 6 and 7 show the lowest speed with no angle as well as the highest speed and angle of attack simulated. The plots for angle of attack of 8° follow like that of no attack where there is a little split in airspeed. This smaller velocity represents the slow moving low-pressure creating drag on the aircraft. However, after an angle of attack of about 10° the grouping of the airspeed between fuselage and horizontal stabilizer becomes tighter. This is better for creating high lift when necessary for ascending elevation.

Table 10: Boundary Conditions of CFD

no. cells	no. nodes	Iteration	Temperature (F)	Density (slug/ft^3)	Dynamic viscous (lbf*s/ft^2)
57378	5748	100	70	0.002341505	3.8E-07

The following Boundary conditions were the properties found within the CFD simulations. There are many cells found in the simulation for a small-scale model which means that there is a greater accuracy for the flows found in the plots of figures 5 and 6. The iterations for the CFD are like those in Figure 3. The following properties were those used for hand calculating drag and lift coefficient. The simulations operate within the same boundary conditions as its comparing data which is only necessary.

Table 11-15: Drag and Lift

Angle of Attack 0				
Speed (ft/s)	Force (Z, lb_f)	Force (Y, lb_f)	Drag Coeff.	Lift Coeff.
30.5392	0.003	0.002	0.454762	0.3031747
62.15944	0.011	0.007	0.4024915	0.256131
98.8463	0.026	0.021	0.3762103	0.3038622

Angle of Attack 8				
Speed (ft/s)	Force (Z, lb_f)	Force (Y, lb_f)	Drag Coeff.	Lift Coeff.
30.5392	0.004	0.01	0.4359702	1.0899254
62.15944	0.014	0.046	0.3683205	1.2101961
98.8463	0.034	0.117	0.3537286	1.2172425

Angle of Attack 15				
Speed (ft/s)	Force (Z, lb_f)	Force (Y, lb_f)	Drag Coeff.	Lift Coeff.
30.5392	0.006	0.017	0.513822	1.455829
62.15944	0.024	0.07	0.4961052	1.4469736
98.8463	0.056	0.179	0.4577664	1.4632177

Angle of Attack 18				
Speed (ft/s)	Force (Z, lb_f)	Force (Y, lb_f)	Drag Coeff.	Lift Coeff.
30.5392	0.007	0.019	0.6544962	1.7764896
62.15944	0.029	0.076	0.6544978	1.7152356
98.8463	0.073	0.193	0.651518	1.7225064

Angle of Attack 24				
Speed (ft/s)	Force (Z, lb_f)	Force (Y, lb_f)	Drag Coeff.	Lift Coeff.
30.5392	0.01	0.019	0.7450903	1.4156715
62.15944	0.039	0.076	0.7014143	1.3668587
98.8463	0.096	0.192	0.6827703	1.3655405

The following five tables represent the 5 angles of attack used for calculating drag and lift forces. Each angle was ran at three different increments representing 30%, 60%, and 100% precent air speed. The following forces were used to calculate corresponding drag and lift coefficients. For an angle of attack of zero, the lift and drag coefficients are similar, however, as the angle increases, the (L/D) ratio ranges from a little below 2 to almost 3. The highest ratio is found in angle of attacks 15° and 18°. As the velocity increased, the (L/D) improved too. These values provide a good range that are representative of the capabilities found from the Embraer C-390.

VIII. Building, Testing and Calculating Drag and Lift Coefficient

In order to test the airplane in the wind tunnel a 3D scale model of it was printed using the MarkForge printer. The model was set to 5 various angles of attack in the wind tunnel with each angle of attack being tested under 3 different wind velocities. From each of these tests, the drag and lift forces were recorded in order to calculate the corresponding coefficients. This allowed us to compare the values from the wind tunnel testing to those found through our simulations and calculations. The following table displays the drag and lift coefficients for each test using the wind tunnel. With the drag, we see a positive correlation between angle of attack and drag coefficient which is true for each wind velocity, excluding the outlier that occurred for the 0 degree angle of attack under 30% wind velocity. The lift coefficients show a slight more complex relationship between angle of attack and lift coefficient. We again see a positive correlation between the two but there are some instances where this is not true.

Table 16: Wind Tunnel Drag and Lift Coefficient

	Wind Tunnel					
	30%		60%		100%	
AOA	Drag Coeff.	Lift Coeff	Drag Coeff.	Lift Coeff	Drag Coeff.	Lift Coeff
0	1.515873	0.340799	0.164524	0.246786	0.260245	0
8	0.340799	0.340799	0.246786	0.904882	0.260245	1.268695
15	0.340799	1.363195	0.329048	1.64524	0.52049	2.081961
18	0.681598	1.363195	0.41131	1.64524	0.683143	2.147022
24	0.681598	1.363195	0.658096	1.398454	1.106042	1.984369

a. Calculated Drag Coefficient

To calculate the drag coefficient for the wings the Shevell approach was used for the wings and fuselage. The following equation resulted in the drag coefficient for the wings and the stabilizers.

$$mac = \frac{2}{3}(C_t + C_r - \frac{C_r C_t}{C_r + C_t})$$

$$Re = \frac{\rho * v * mac}{\mu}$$

$$S_{wet} = 2(1 + \frac{0.2t}{c})$$

$$\overline{C_f} = \frac{0.455}{(log_{10}Re)^{2.58}} - \frac{1700}{Re}$$

$$C_D = \frac{k * \overline{C_f} * S_{wet}}{\frac{1}{2}\rho v^2 S}$$

Table 17: Wing

Speed	mac	Re	S_{wet}	$\bar{c}_f$	C_{Do}
30%	0.541923	8.5E+03	2.048	1.3E-02	1.6E-02
60%	0.541923	1.7E+04	2.048	1.1E-02	1.3E-02
100%	0.541923	2.8E+04	2.048	9.9E-03	0.0114538

Table 18: Horizontal Stabilizer

Speed	mac	Re	$\bar{c}_f$	C_{Do}
30%	0.068	1.3E+04	1.2E-02	1.2E-02
60%	0.068	2.6E+04	9.9E-03	1.0E-02
100%	0.068	4.1E+04	8.8E-03	9.2E-03

Table 19: Vertical Stabilizer

Speed	mac	Re	$\bar{c}_f$	C_{Do}
30%	0.0618	1.2E+04	1.2E-02	1.5E-02
60%	0.0618	2.4E+04	1.0E-03	1.2E-02
100%	0.0618	3.8E+04	9.0E-03	1.1E-02

A similar approach was used for the fuselage. The following equations were used.

$$Re = \frac{\rho * v * L}{\mu}$$

$$S_{wet,nose} = 0.75\pi D L_{nose}$$

$$S_{wet,body} = \pi D L_{body}$$

$$S_{wet,tail} = 0.72\pi D L_{tail}$$

$$S_{wet,total} = S_{wet,nose} + S_{wet,body} + S_{wet,tail}$$

$$\overline{C_f} = \frac{0.455}{(log_{10}Re)^{2.58}} - \frac{1700}{Re}$$

$$C_D = \frac{k * \overline{C_f} * S_{wet}}{S_{ref}}$$

Table 20: Fuselage

Speed	$S_{wet,total}$	Re	$\bar{c}_f$	C_{Do}
30%	7.122029	691813.8	0.161033	0.920906
60%	7.122029	1408117	0.157472	0.90054
100%	7.122029	2239195	0.15498	0.886292

b. Calculated Lift Coefficient

The process to calculate the lift coefficient of the aircraft is shown below.

$$a_o = \frac{c_l}{\alpha - \alpha_{L=0}}$$

$$a = \frac{a_o}{1 + \frac{a_o}{\pi ARe}}$$

$$C_L = a(\alpha - \alpha_{L=0})$$

Table 21: Lift Coefficient at Different Angle of Attacks

aoa	$\alpha_{L=0}$	C_l	α	a_o	a	C_L
0	-4.95	1.4	1.5	0.070175	0.053034	0.262518
8	-4.95	1.4	1.5	0.070175	0.053034	0.68679
15	-4.95	1.4	1.5	0.070175	0.053034	1.058027
18	-4.95	1.4	1.5	0.070175	0.053034	1.217129
24	-4.95	1.4	1.5	0. 070175	0.053034	1.53353

Table 22: Calculated Drag and Lift Coefficient

	Calculated Coefficients					
	30%		60%		100%	
aoa	Drag Coeff.	Lift Coeff	Drag Coeff.	Lift Coeff	Drag Coeff.	Lift Coeff
0	2.019773	0.262518	1.949129	0.262518	1.904877	0.262518
8	2.052148	0.68679	1.981504	0.68679	1.937251	0.68679
15	2.104214	1.058027	2.03357	1.058027	1.989318	1.058027
18	2.13331	1.217129	2.062667	1.217129	2.018414	1.217129
24	2.203712	1.535333	2.133068	1.535333	2.088816	1.535333

The following graphs illustrate the relationship between Lift & Dag coefficients at different angles of attack. For all graphs, we can see that as the angle increases, so do the coefficients. Lift increases at a much quicker rate than drag, however it begins to plateau and decrease after an angle of attack of about 18°. The drag coefficient only varies about 0.5 but it generally increases over every angle of attack. For all airspeeds, we can see similar patterns for all three coefficients. When analyzing the drag coefficients, the Hand Calculated values are usually more than two times greater compared to the CFD and Wind Tunnel values; the CFD and Wind Tunnel behave very similarly. All three lift coefficients generally follow the same pattern with the highest values found first in the Wind Tunnel followed by CFD and then the Hand Calculations. Considering the range of values that each of the three tests provide, it is reassuring to see that all three tests begin and end with similar values.

Figure 8A and 8B: Lift and Drag coefficients at different angles of attack [30% airspeed]

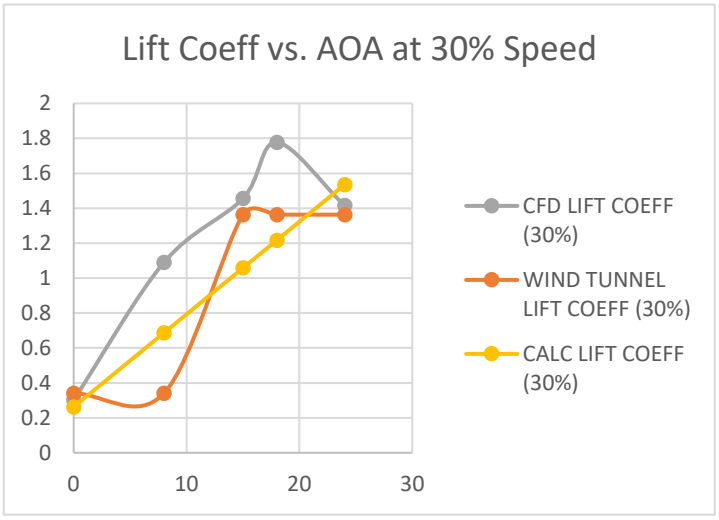

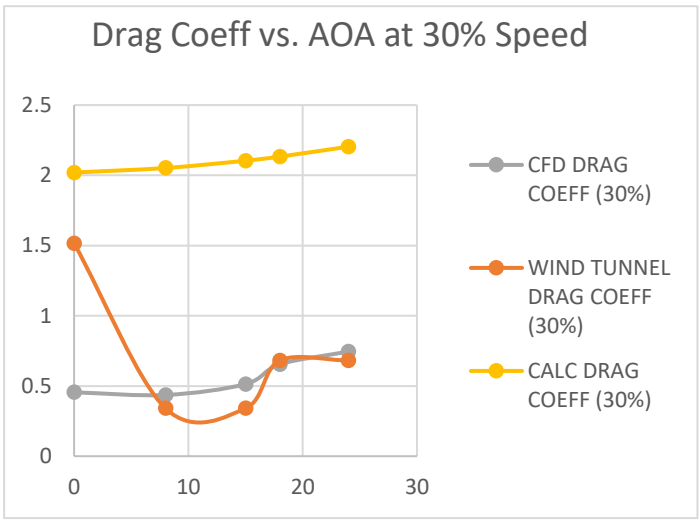

As shown before, low speeds do not produce much pressure difference around the plane for necessary lift and drag, so the change in geometry with each angle of attack makes huge differences as shown above. Around an angle of 10° we can see that both lift and drag

coefficients found in the wind tunnel start to shift from decreasing to increasing. The other two tests have more consistent performance.

Figure 9A and 9B: Lift and Drag coefficients at different angles of attack [60% airspeed]

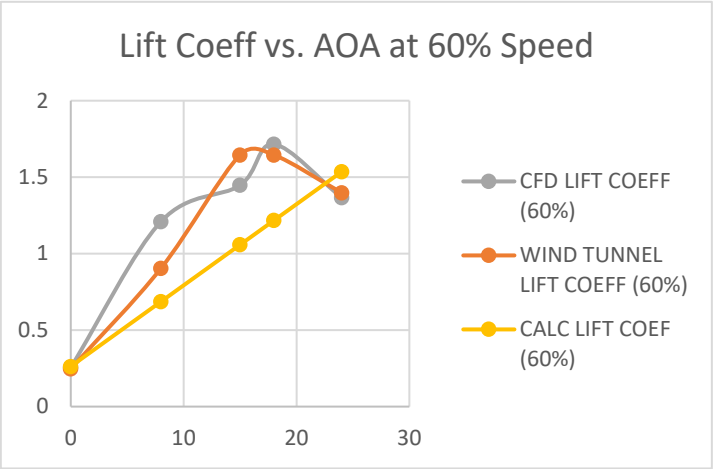

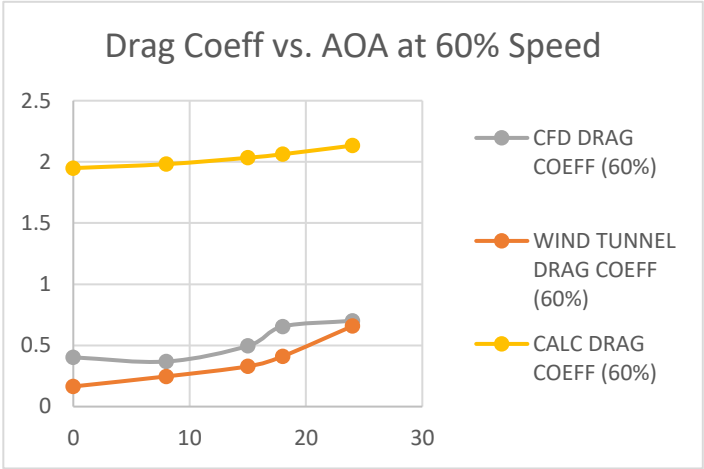

60% airspeed has the tightest grouping for data for the three different air speeds tested. This is reassuring because we know that there is a speed where we have more confidence in the aircraft's projected ability to produce adequate Lift and Drag. This airspeed shows the smallest range in values at the highest angle of attack which further confirms that we have a representative range of data for these boundary conditions.

Figure 10A and 10B: Lift and Drag coefficients at different angles of attack [100% airspeed]

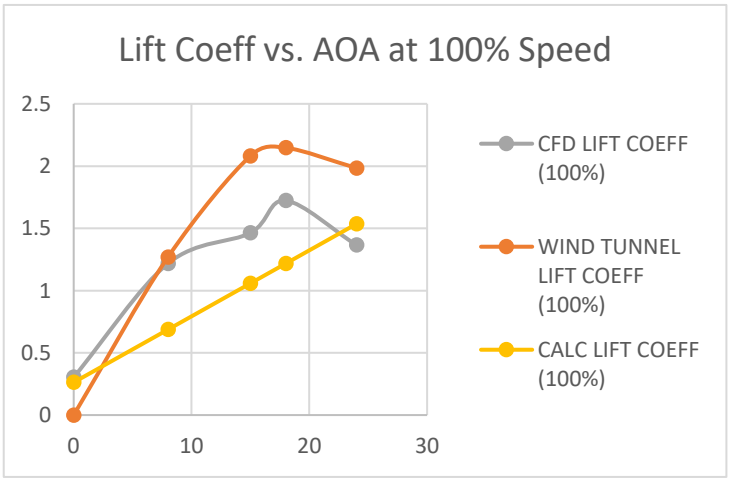

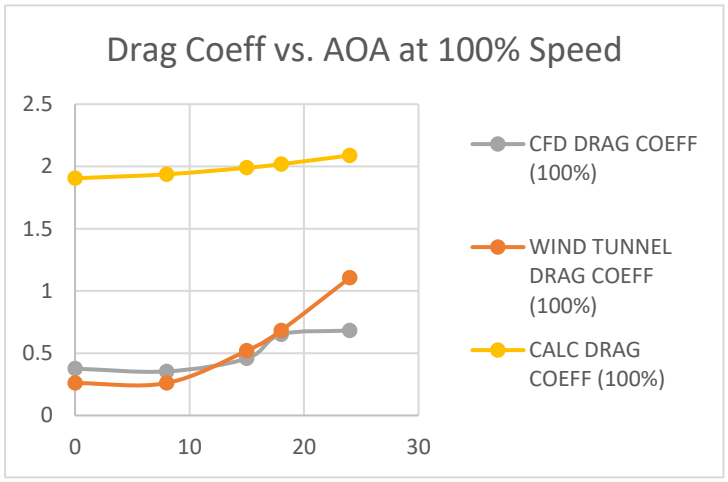

The max airspeed doesn't reveal anything that we haven't already seen before. But it is important to notice that the CFD and the Wind Tunnel coefficients start to split in values. For each previous airspeed these two tests usually end together, but with 100% airspeed the see the Wind Tunnel start to produce more lift around 20° angle of attack.

Conclusion

An Introduction to Aerodynamics well done. The aim to further understand fundamental physical quantities and the source of Aerodynamic forces was assisted by breaking down our Embraer C-390 aircraft piece by piece and measuring the rudimentary elements of airplane performance. The first component accounted for was the weight. The coded iterative process calculated a weight that was 30,000 pounds heavier than the initial guess of 163,000 lbs. The 30K difference was not outlandish as the initial guess did not account for any cargo other than crew and average fuel weight. The C-390 is known to push 200,000 lbs for max load which lets us know the 30K difference provides a good average for flight performance. Characteristics such as wing and fuselage dimensions were calculated with equations, tables, and charts that were gracefully provided by our profesora. The fuselage area, length, and diameter were found in English units; the wingspan, chord length and root vs tip aspect ratio were calculated using the respective tools. In another section of this report, the same measurements were calculated for the horizontal and vertical stabilizers.

All physical bodies of the aircraft were modeled and mated together for empirical testing of the plane's elements in Wentworth Institute of Technology's wind tunnel provided in the fluid's lab. The results from the wind tunnel were recorded in SI units and compared to SolidWorks CFD fluid simulation. The simulations were evaluated in the same boundary conditions as the empirical data and gave data such as drag and lift which were used to compare to theoretical values found when analyzing the wings in section three. In the final section, we finally get a comparison of all the values calculated throughout the process of quantifying the elements of the Embraer C-390. Lift and drag coefficients were two parameters used to differentiate CFD, wind tunnel, and hand calculations performance. In the end, the three methods used provide a representative range of expected aircraft capabilities over different applied angle of attacks. All three lift coefficients usually behaved similarly over the range of attacks, however, there is a noticeable difference in the wind tunnel producing consistent better results than the hand calculations found earlier in the research. As for the drag coefficient, the hand calcs produced results sometimes two times greater than the wind tunnel or CFD. This is initially upsetting seeing the agreements in methods for lift, but still we are provided with values that provide a small scope of theoretical and tested data that can explain what to expect from and aircraft shaped and built like the Embraer C-390.

It is a lot to consider when testing and analyzing multiple methodologies at once, but we were taught well how to sort the information. Sometimes there are pieces applicable to all data and that's results. The lift and drag coefficients encompass all components of the aircraft's form such as geometry, flight conditions and patterns. The goal of understanding the basics of aerodynamics was surpassed into something much more valuable.

Reference:

[1] Valpolini, Paolo., April 28 2023, "LAAD 2023- Embraer strongly pushes its C-390 Millennium on the international market", *European Defence Review On-Line* https://www.edrmagazine.eu/embraer-strongly-pushes-its-c-390-millenium-on-the-international-market

[2] Chen, Michael Chien-Wei., 2014, "Commercial Viability Analysis of Lignin Based Carbon Fiber", *Simon Fraser University* https://summit.sfu.ca/item/14423

[3] Vinholes, Thiago,. April 22 2023, "Which Countries Can Order The Embraer KC-390 Millennium?" *Air Data News* https://www.airdatanews.com/which-countries-can-order-the-embraer-kc-390-millennium/

[4] "Embraer KC-390." *Encyclopedia*, 31 Oct. 2022, encyclopedia.pub/entry/32066.

[5] Aviation Week Network, March 30 2022, "C-390 Millennium. The New Generation Airlifter, For Today's World" *Defense and Space*, https://aviationweek.com/defense-space/multi-mission-aircraft/c-390-millennium-new-generation-airlifter-todays-world

[6] "Embraer: C-390 Millennium." Portal Embraer, defense.embraer.com/global/en/c-390.